

OmniZip: Learning a Unified and Lightweight Lossless Compressor for Multi-Modal Data

Yan Zhao¹, Zhengxue Cheng^{1*}, Junxuan Zhang², Dajiang Zhou², Qunshan Gu², Qi Wang², Li Song^{1*}

¹Shanghai Jiao Tong University ²Ant Group

¹{zhaoyanzy, zxcheng, song_li}@sjtu.edu.cn

²{junxuan.zjx, dajiang.zdj, qunshan.gu, qw.qq}@antgroup.com

Abstract

*Lossless compression is essential for efficient data storage and transmission. Although learning-based lossless compressors achieve strong results, most of them are designed for a single modality, leading to redundant compressor deployments in multi-modal settings. Designing a unified multi-modal compressor is critical yet challenging, as different data types vary largely in format, dimension, and statistics. Multi-modal large language models offer a promising resolution but remain too complex for practical use. Thus, we propose **OmniZip, a unified and lightweight lossless compressor for multi-modal data (like image, text, speech, tactile, database, and gene sequence)**. Built on a lightweight backbone, OmniZip incorporates three key components to enable efficient multi-modal lossless compression: a modality-unified tokenizer that reversibly transforms diverse data into tokens, a modality-routing context learning mechanism that enables flexible multi-modal context modeling, and a modality-routing feedforward design that further enhances the model’s nonlinear representation flexibility. A reparameterization training strategy is used to enhance model capacity. OmniZip outperforms or matches other state-of-the-art compressors on multiple modalities, achieving 42%, 57%, 62% and 42%, 53% higher compression efficiency than gzip on CLIC-M, TouchandGo, enwik9, LibriSpeech, and WikiSQL datasets, respectively. It also supports near real-time inference on resource-constrained edge devices, reaching about 1MB/s on MacBook CPUs and iPhone NPUs. Our code is released at <https://github.com/adminasmi/OmniZip-CVPR2026>.*

1. Introduction

According to information theory [60], the optimal code length for a symbol is determined by its negative logarithmic probability. This insight motivates the modern lossless

compression strategy: use probabilistic models to estimate data likelihoods and apply entropy coding [26, 33, 34] to encode data. Recent approaches further leverage neural networks and large language models (LLMs) to improve probability estimation and enhance compression performance [9, 13, 15, 22, 24, 32, 42, 44, 46, 64, 67, 71, 74, 75].

Despite recent progress, learning-based lossless compression faces two key challenges.

- *First, many existing methods, especially those based on LLMs [13, 22, 24, 64], suffer from excessive complexity.* These models often contain billions of parameters, far exceeding the size of compressed data. Since compression speed is decided by the model’s inference speed, such complexity severely limits these methods’ practical deployments. For example, compressing a single 1080p image using LLaMA3-8B [3] takes over 30 minutes [13, 24], while [8, 38] need several days to compress 1 GB of text.
- *Second, most existing methods are designed for a single modality [5, 13, 64, 71], necessitating separate compressors in multi-modal systems.* This increases software complexity and hardware costs. Despite its importance, multi-modal lossless compression remains challenging due to the heterogeneity of modalities: text is discrete and sequential, images are two-dimensional and spatially organized, speech is continuous with smooth spectral patterns, database contains structured categorical fields, and gene sequences exhibit symbolic structures with characteristic motifs. Some works [22] explore multi-modal lossless compression by converting all data to ASCII text, causing sub-optimal performance on non-text modalities.

To tackle these challenges, we propose **OmniZip**, a unified and lightweight lossless compressor for multi-modal data. It supports most real-world data types suitable for lossless compression: image-like data (e.g., natural image, medical image, tactile signals), text-like data (e.g., natural language, gene sequence, database), and speech. Built upon a lightweight backbone, OmniZip explicitly addresses modality heterogeneity and enables efficient multi-modal compression through three key designs: (1) *a modality-*

*Corresponding author.

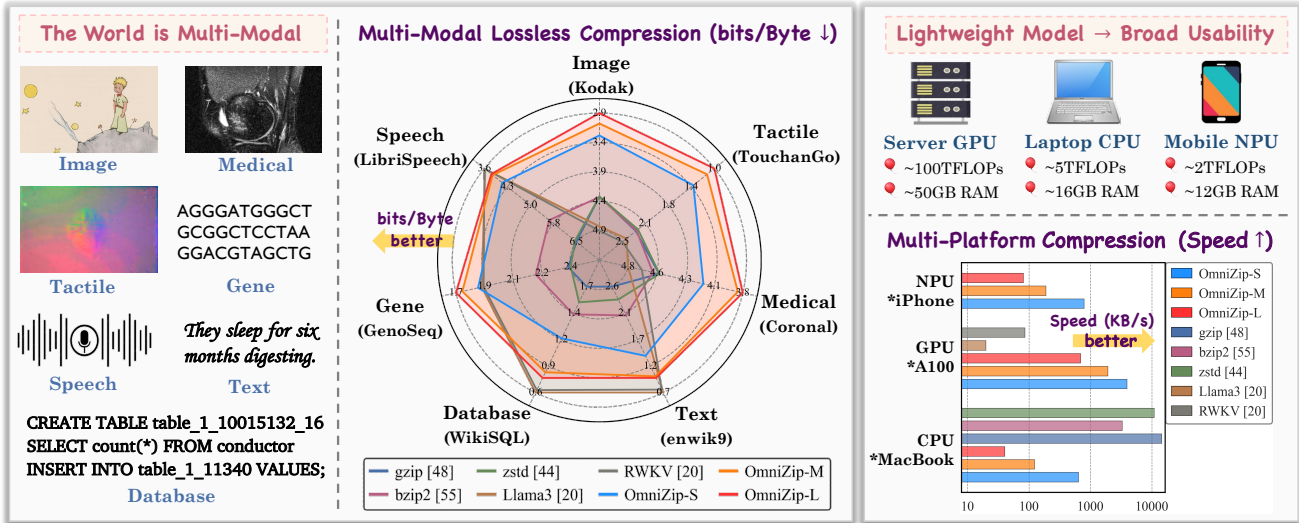


Figure 1. **Left:** The world is multi-modal, motivating the need for unified lossless compression. Multi-modal compressors’ performance is shown across modalities, where points closer to the edge indicate better efficiency (lower bits/Byte). **Right:** Lightweight design ensures broad usability across platforms. OmniZip achieves near real-time inference (hundreds of KB/s to MB/s) even on edge devices.

unified tokenizer that maps diverse data into a unified and fully reversible token space, (2) *a modality-routing context learning mechanism* that enables flexible multi-modal context modeling, and (3) *a modality-routing feedforward process* that introduces adaptive feedforward representations. A *reparameterization training strategy* further enhances the model capacity without increasing the inference cost.

With much fewer parameters, OmniZip matches or surpasses the SOTA compressors across diverse modalities. It supports deployment across CPUs, NPUs, and GPUs, achieving near real-time inference even on resource-constrained edge devices (e.g., laptops and mobile phones).

Generally, our contributions can be concluded as:

- We propose OmniZip, a unified and lightweight lossless compressor for multi-modal data. It supports efficient lossless compression for image-like (natural image, medical image, tactile signal), text-like (natural language, gene sequence, database), and speech data. OmniZip explicitly addresses modality heterogeneity and provides useful insights for the emerging multi-modal applications.
- Built on a lightweight backbone, OmniZip integrates three key techniques for efficient multi-modality lossless compression: modality-unified tokenization, modality-routing contextual learning, and modality-routing feed-forward. A reparameterization training strategy is also employed to enhance the model’s capacity.
- We evaluate OmniZip on 16 datasets across seven modalities. It outperforms or matches other SOTA compressors, achieving 42%, 57%, 62% and 42%, 53% higher compression efficiency than gzip on CLIC-M, TouchandGo, enwik9, LibriSpeech, and WikiSQL datasets. Even on edge devices like MacBook CPU or iPhone NPU, OmniZip reaches near real-time inference (0.1~1MB/s).

2. Related Work

Classical Lossless Compressors. Classical lossless compression can be broadly categorized into general-purpose and modality-specific approaches. General-purpose compressors such as gzip [52], bzip2 [59], and zstd [48] operate across diverse data types without domain-specific assumptions. Gzip integrates LZ77 [76] and Huffman coding [34], bzip2 builds on the Burrows-Wheeler transform [45] and move-to-front encoding [4], while zstd uses fast LZ-style matching along with finite-state entropy coding [30].

Modality-specific compressors, in contrast, leverage domain-specific statistical structures for higher efficiency. For images, codecs like PNG [11], WebP [29], FLIF [62], JPEG XL [63], JPEG 2000 [37], and BPG [7] exploit spatial redundancy with filtering, prediction, or transform coding. For lossless speech compression, FLAC [18] uses linear predictive coding to model waveforms and compresses the residual signals with entropy coding.

Learning-based Lossless Compressors. Learning-based compression has progressed rapidly in both lossy [14, 25, 27, 40, 41, 66] and lossless domains [5, 22, 32, 42, 46, 67, 69, 71]. We focus on lossless compression, which combines probability prediction with entropy coding to achieve bit-exact reconstruction. These methods are typically designed for a single modality, as the statistical properties of images, text, and speech differ greatly, making cross-modality generalization challenging. Existing text compressors use auto-regressive architectures to model token sequences [8, 9, 38, 49, 64, 71], while image compressors attempt to capture the spatial dependencies [5, 13, 24, 46, 47, 72, 73]. While [22, 32] explore multi-modal lossless compression, they treat all modalities as byte or ASCII text, overlook-

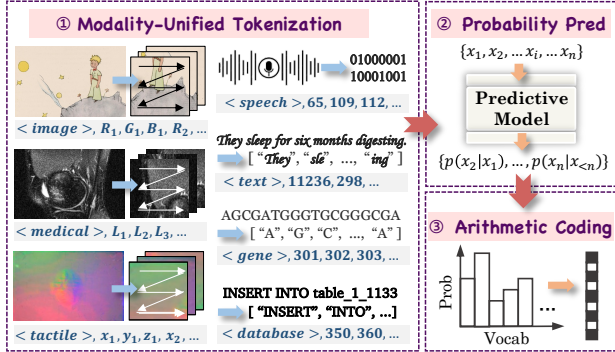


Figure 2. Overview of the proposed OmniZip framework. Diverse data is first converted into a unified, fully reversible token space. A predictive model then estimates each token’s contextual probability, followed by arithmetic coding to generate the bitstream.

ing the modality heterogeneity and leading to sub-optimal performance. In addition, learning-based compressors, especially those built upon LLMs [9, 13, 22, 24, 49, 64], often suffer from heavy computational complexity.

3. Proposed Method

As outlined in Fig. 2, OmniZip enables lossless compression for multiple modalities, supporting image-like data (natural image, medical image, tactile signal), text-like data (natural language, gene sequence, database), and speech. Input data is first converted into tokens $\{x_1, x_2, \dots, x_n\}$ through a modality-unified tokenizer. A predictive model estimates each token’s contextual probability $p(x_i|x_{<i>i</i>})$. Then, arithmetic coding (AC) [33] encodes the data towards its entropy bound $H(p) = \mathbb{E}(\sum_{i=1}^n -\log_2 p(x_i|x_{<i>i</i>}))$.

3.1. Preliminaries: Low-Complexity Backbone

Parameter-Efficient Prediction Model. To lay a foundation for efficient compression, we compare three common backbones of prediction models: Transformer [65], Mamba [31], and RWKV [54]. They are evaluated based on compression performance (bits/Byte), computational cost (MACs), and inference speed (KB/s) on a MacBook CPU. For simplicity, we focus on text compression for model selection and do not consider multi-modal data.

Specifically, text data is tokenized using SentencePiece BPE tokenizer [58] (vocabulary size is 16K), and then split into token sequences of length 1024 for model input. The three models perform auto-regressive next-token probability prediction, with arithmetic coding applied to generate the compressed bitstream. All models are trained on enwik8 [19] and evaluated on enwik9 [20]. As shown in Tab. 1, under such lightweight model settings, RWKV achieves the best balance of compression efficiency and inference speed, making it the preferred backbone. The Mamba model, after adaptation for CPU compatibility, exhibits relatively slow inference and is thus excluded from further comparisons.

Table 1. Comparison for model backbone selection. Models are evaluated using text lossless compression. Inference speed is measured on the MacBook Pro CPU, with a batch size of 128.

Model	#Params ↓	MACs ↓	bits/Byte ↓	Speed (KB/s) ↑
Transformer [65]	0.2M	0.88M	2.197	714
	3.2M	4.43M	1.984	280
RWKV-7 [54]	0.2M	0.85M	1.910	2292
	3.2M	3.68M	1.658	856

Reparameterization Training Strategy. Inspired by [71], we employ a reparameterization strategy [23] to enhance the model’s performance without affecting inference speed. During training, additional branches are added to increase the model’s capacity. These branches are then merged back into the main path during inference, ensuring that inference complexity remains unchanged. Following [71], we apply reparameterization to the receptance (R), key (K), and value (V) layers in the Time Mixing module of RWKV. To further increase the training capacity, we apply high-rank matrix decomposition to the added branches [71].

3.2. Modality-Unified Tokenization

To enable lossless compression across diverse modalities, we design a unified tokenization strategy that can reversibly represent diverse data within a unified token space. The key challenge lies in the structural and statistical differences among modalities: for instance, images are two-dimensional with 8-bit RGB sub-pixels, text is discrete and highly variable, and speech is continuous with smooth temporal patterns. Furthermore, the tokenization must remain fully invertible to ensure lossless compression.

Specifically, we group data into three categories: image-like data, text-like data, and speech. For text-like data (natural language, gene, and database), we follow [71] and use a SentencePiece BPE tokenizer with a 16K vocabulary. To further improve efficiency, domain-specific symbols are explicitly added to the vocabulary, including nucleotide bases (A, T, G, C) for gene sequences and common script keywords (e.g., “select”, “or”, “and”) for databases.

For image-like data, including natural images, medical images, and tactile signals, we first divide each image into $16 \times 16 \times 3$ patches to preserve local spatial correlations. Within each patch, pixels are flattened in a raster-scan order, and each pixel’s RGB values are sequentially expanded as sub-pixels $(R_1, G_1, B_1, R_2, G_2, B_2, \dots)$. Each sub-pixel is treated as an individual token, yielding a vocabulary of size 256. Tactile images captured by visual sensors are processed like natural images, while tactile force data are mapped from 3D (x, y, z) signals into RGB images for tokenization. For medical images that are typically grayscale, each pixel intensity is treated as a single token.

For speech data, which is inherently continuous and difficult to discretize without loss, we directly read the

raw byte stream and treat each byte as a token, also producing a 256-size vocabulary. By merging each modality’s vocabulary, we create a unified token set for probability prediction. To help the model better distinguish between different modalities, we prepend each token sequence with a modality-specific prefix, i.e., <image>, <medical>, <tactile>, <text>, <gene>, <database>, or <speech>.

Before softmax and arithmetic coding, modality masking is applied to zero out probabilities of non-target modalities, thereby reducing estimation errors and enhancing compression efficiency. For instance, when compressing images, only image-related token probabilities are retained.

3.3. Modality-Routing Context Learning

In our RWKV backbone, each block consists of two components: a Time Mixing module [54] and a multilayer perceptron (MLP) [57]. The Time Mixing module models contextual dependencies through operations like token shift, R/K/V projection, WKV calculation, and state updates.

As shown in Fig. 2, different modalities exhibit distinct contextual dependencies. To enhance multi-modal processing, we integrate a mixture-of-experts (MoE) mechanism [12] into the Time Mixing module. Considering computational efficiency, we experiment with applying MoE to different components and find that applying MoE to the V layer yields impressive results. This phenomenon may stem from the inherent mechanism that, while the K layer serves as a semantic index and the R layer functions as a memory gating, the V layer represents the specific memory content. The diversity within the V layer is more crucial in handling multi-modal data. Therefore, we apply MoE only to the V layer, with the K and R layers shared across all V experts.

Specifically, as shown in Fig. 3, a learnable router assigns each token x_i a score $g_{i,e}$ for each expert e :

$$g_{i,e} = \text{softmax}(x_i W_g)_e = \frac{\exp(x_i W_{g,e})}{\sum_{e'=1}^E \exp(x_i W_{g,e'})}, \quad (1)$$

where W_g is the routing projection and E is the number of experts. Experts with the top- k scores then process the token. Herein, each expert is a V projection layer, and the router is a small feedforward network. The final output is the weighted sum of the selected experts’ outputs:

$$V(x_i) = \sum_{e \in \text{top-}k} \hat{g}_{i,e} \cdot e(x_i) \quad (2)$$

where $e(x_i)$ denotes the output of expert e for token x_i , and $\hat{g}_{i,e}$ is the re-normalized score. To ensure a compact model design, we experimentally use 4 experts, with top- k set to 2. This only adds the computational and parameter overhead of 3 additional V layers per Time Mixing module, which is negligible compared to the entire model.

3.4. Modality-Routing Feedforward Process

In RWKV, each block integrates a feedforward MLP to enhance the nonlinear representations [54]. However, using

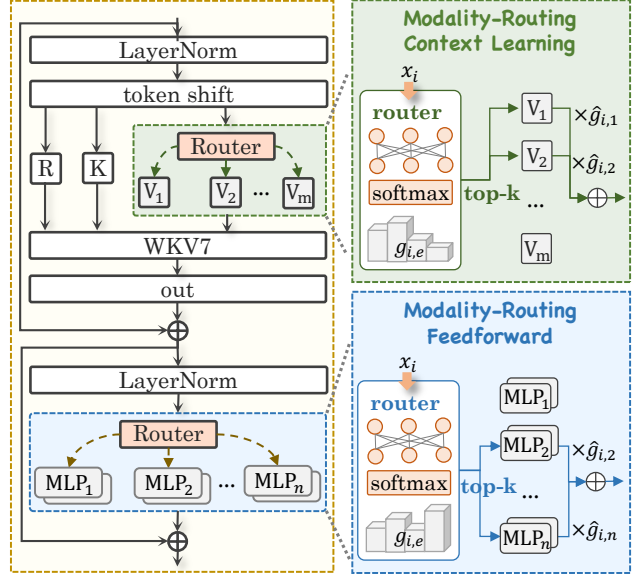


Figure 3. One block of OmniZip’s predictive model. The model stacks N such blocks in total. Built on a lightweight RWKV7 backbone, it incorporates two modality-routing MoE modules for contextual learning and feedforward processing.

a general-purpose MLP is not well-suited for multi-modal processing, as it lacks the flexibility to effectively capture the distinct characteristics of different modalities.

To better support multi-modal compression, we replace it with an MoE-based modality-routing feedforward module, as shown in Fig. 3. The routing strategy follows Sec. 3.3, except that the experts here are small MLPs instead of V projection layers. Each MLP expert uses a hidden factor of $2\times$, half that of the original large MLP. With four experts and top- $k = 2$, the number of activated parameters per token is roughly the same as the original MLP, while the MoE design offers greater flexibility for multi-modal processing.

3.5. Loss Function

Our loss function consists of two parts: (1) a primary cross-entropy loss that measures the divergence between the predicted and target distributions, and (2) auxiliary regularization terms that stabilize mixture-of-experts training, including the router Z-loss [77] and the load-balancing loss [61].

$$\begin{aligned} \mathcal{L} = & \underbrace{-\sum q \log p}_{\text{Cross Entropy}} \\ & + \lambda \underbrace{\frac{1}{T} \sum_{j=1}^T \left(\log \sum_{t=1}^N e^{x_{i,t}} \right)^2}_{\text{Z-loss}} \\ & + \mu \left[\underbrace{CV^2 \left(\sum g_{i,e} \right)}_{\text{Expert Importance}} + \underbrace{CV^2 \left(\sum \mathbb{I}(g_{i,e} > 0) \right)}_{\text{Load Balance}} \right] \end{aligned} \quad (3)$$

As shown in Eq. (3), the Z-loss penalizes large logits in the gating network, preventing instability during routing.

ing and accelerating convergence. The auxiliary loss encourages balanced expert utilization by penalizing the variance in expert importance and token assignment, where CV^2 denotes the squared coefficient of variation [1], and $\mathbb{I}(g_{i,e} > 0)$ is the indicator of expert selection. The loss terms are weighted using $\lambda = 0.001$ and $\mu = 0.01$.

4. Experiments

4.1. Experimental Setup

Implementation Details. We vary the model size by adjusting the embedding dimension and the number of blocks, creating three model variants: *OmniZip-S*, *OmniZip-M*, and *OmniZip-L*, as shown in Tab. 2.

Table 2. Details of the proposed OmniZip models.

Model	Blocks	Embed Dim	#Params	MACs
OmniZip-S	2	320	4.8M	3.88M
OmniZip-M	2	912	38M	18.2M
OmniZip-L	3	1488	152M	56.0M

The models are trained using the FusedAdam optimizer [50] with a *three-stage training strategy* to stabilize the optimization of mixture-of-experts: (1) freeze the feedforward routing module and train the remaining parameters for two epochs with a learning rate of 1×10^{-4} ; (2) freeze the contextual routing module and train the other components for another two epochs with a learning rate of 1×10^{-4} ; (3) unfreeze all parameters and train the entire model for 20 epochs using a cosine annealing learning rate scheduler [43], starting at 1×10^{-4} and decaying to 1×10^{-5} . All training process is conducted on NVIDIA A100 GPUs.

Multi-Modality Datasets. Our dataset covers seven types: natural image, medical image, tactile signal, text, gene sequence, database, and speech. In total, 16 datasets are utilized for training and evaluation:

- **Image:** we train on the training set of DIV2K [2], and evaluate on Kodak [21], CLIC-Pro, CLIC-Mobile [17], and the test set of DIV2K.
- **Medical:** we adopt MRNet Axial, Coronal, and Sagittal datasets [10] and follow their official train–test splits.
- **Text:** the training set consists of enwik8 [19] and 2000 Gutenberg eBooks [56]. The test set is enwik9 [20] and additional 1000 Gutenberg eBooks.
- **Speech:** we use the LibriSpeech dataset [51] with its official training and test splits.
- **Database:** we train on the Spider training set [70], and evaluate on both WikiSQL [35] and the Spider test set.
- **Gene:** we use GenoSeq [16] and DNACorpus [55] datasets, and follow their official train-test splits.
- **Tactile:** the training and test sets follow the official partitions of TouchandGo [68] and ObjectFolder [28].

To ensure balanced training across modalities, we control each modality’s training set to 1GB via random sampling and data augmentation. Further, we also implement a

balanced batch sampler to ensure even sampling from each modality in every batch by cycling through shuffled indices.

Compared Methods and Metrics. We compare lossless compression across different modalities. Classical baselines include general-purpose lossless compressors (gzip [52], bzip2 [59], zstd [48]), image-specific compressors (PNG [11], WebP [29], FLIF [62], JPEG XL [63], JPEG2000 [37], BPG [7]), and the speech lossless compressor FLAC [18]. For learning-based methods, we evaluate recent image lossless compressors [5, 13, 42, 46, 47, 67], text compressors [8, 9, 38, 71], and multi-modal compressors [22] which compresses data using pretrained LLMs [3, 53]. Herein, image-like data (natural images, medical images, and tactile data) can be compressed using image and general-purpose compressors, while text-like data (natural language, gene, and databases) are compressed using text and general-purpose compressors. There is currently no dedicated learning-based lossless speech compressor.

We evaluate compression performance using bits/Byte as metrics. Model complexity is assessed by MACs and inference speed (KB/s) on multiple devices (an NVIDIA A100 GPU, a MacBook Pro CPU, and an iPhone 17 Pro NPU).

4.2. Multi-Modality Lossless Results

Tab. 3 and Tab. 4 compare OmniZip with existing lossless compression methods. The former reports results on image-like data (natural image, medical image, and tactile data), while the latter presents results on text-like data (natural text, gene sequence, database) and speech. Both tables include general-purpose multi-modal compressors (colored in gray) and modality-specific compressors for comparison. The radar chart in Fig. 1 compares multi-modal compressors across different modalities, while Fig. 4 offers comparisons of learning-based compressors on individual datasets.

Compression Results on Image-like Data. As shown in Tab. 3, general-purpose classical compressors such as gzip, bzip2, and zstd show limited effectiveness on image-like data, achieving about 4.3, 2.3, 4.6 bits/Byte on Kodak, TouchandGo, and Coronal, respectively. Among classical image compressors, FLIF and JPEG-XL perform the best, offering roughly $1.5 \times \sim 2.5 \times$ better compression than gzip.

Learning-based methods exhibit clear domain dependency. DLPR, L3C, RC, and P2LLM, all trained on natural images, perform worse on tactile and medical data. Though Deletang et al. [22] presents as a general-purpose compressor, it compresses images by converting them into ASCII sequences and applying pretrained LLMs [3, 53] for probability prediction, resulting in sub-optimal performance.

In contrast, OmniZip achieves pleasing compression across all image-like modalities. Even the smallest version, OmniZip-S, performs comparably to specialized learning-based methods and outperforms gzip by about 30% on medical, tactile, and natural images. OmniZip-M and OmniZip-

Table 3. Lossless compression results on image-like (natural image, medical image, and tactile) datasets. Multi-modal compressors (except ours) are shown in gray. * denotes pretrained LLMs, † indicates that some results are reproduced by us. / indicates compression speeds measured on a MacBook CPU, and ‡ denotes speeds on an A100 GPU (batch size 128). Other unmarked values are taken from their papers.

Compressor	#Params↓	MACs↓	Speed (KB/s)↑	Multi Modal	bits/Byte↓									
					Kodak	CLIC-P	CLIC-M	DIV2K	TouchandGo	ObjectFolder	Axial	Coronal	Sagittal	
Classical	gzip† [52]	-	-	14500′	✓	4.349(0%)	4.039(0%)	3.947(0%)	4.224(0%)	2.298(0%)	3.969(0%)	5.346(0%)	4.563(0%)	5.571(0%)
	bzip2† [59]	-	-	3300′	✓	4.359	4.033	3.931	4.208	2.288	4.031	5.403	4.617	5.628
	zstd† [48]	-	-	11000′	✓	4.350	4.042	3.952	4.229	2.263	3.966	5.343	4.560	5.568
	PNG† [11]	-	-	200′	✗	4.349	4.041	3.952	4.229	2.500	3.964	5.361	4.581	5.580
	FLIF† [62]	-	-	652′	✗	2.903	2.792	2.497	2.914	0.808	3.765	4.860	3.999	5.160
	BPG† [7]	-	-	180′	✗	3.382	3.144	2.855	3.285	0.936	3.726	5.004	4.167	5.337
	WebP† [29]	-	-	330′	✗	3.205	3.006	2.774	3.176	0.739	3.612	4.944	4.161	5.214
	JPEG-XL† [63]	-	-	970′	✗	2.902	2.722	2.395	2.826	0.739	3.657	4.719	3.891	5.091
	JPEG2000† [37]	-	-	5000′	✗	3.301	2.927	2.667	3.127	1.552	3.989	5.019	4.170	5.310
Learning-based	Llama3*† [22]	8B	7.80G	20‡	✓	4.862	4.290	4.234	4.378	2.455	4.060	5.514	4.832	5.784
	RWKV*† [22]	7B	7.19G	86‡	✓	4.937	4.310	4.298	4.718	2.523	4.118	5.244	4.712	5.529
	DLPR*† [5]	22.3M	-	640	✗	2.860	2.380	2.160	2.550	1.082	3.774	-	-	-
	L3C*† [46]	5M	6.86M	178	✗	3.260	2.940	2.640	3.090	1.350	3.842	5.160	4.450	5.520
	RC [47]	-	-	-	✗	-	2.930	2.540	3.080	-	-	-	-	-
	P2LLM [13]	8B	-	20‡	✗	2.830	2.350	2.080	2.510	-	-	-	-	-
	aiWave [67]	695M	-	40	✗	-	-	-	-	-	-	4.550	3.800	4.830
	BCM [42]	12.5M	-	-	✗	-	-	-	-	-	-	4.410	3.630	4.810
Ours	OmniZip-S	4.8M	3.88M	1223‡	✓	3.307(-24%)	2.933(-27%)	2.620(-34%)	2.968(-30%)	1.338(-42%)	3.275(-18%)	4.560(-15%)	4.179(-8%)	5.286(-5%)
	OmniZip-M	38M	18.2M	1015‡	✓	3.103(-29%)	2.926(-28%)	2.378(-40%)	2.749(-35%)	1.110(-52%)	2.973(-25%)	4.531(-15%)	3.880(-15%)	4.969(-11%)
	OmniZip-L	152M	56.0M	420‡	✓	2.925(-33%)	2.578(-36%)	2.273(-42%)	2.542(-40%)	0.987(-57%)	2.689(-32%)	4.466(-16%)	3.837(-16%)	4.848(-13%)

Table 4. Lossless compression results on text-like (natural text, gene sequence, database) and speech datasets. Multi-modal compressors (except ours) are shown in gray. * denotes pretrained LLMs, † indicates that some results are reproduced by us. / indicates compression speeds measured on a MacBook CPU, and ‡ denotes speeds on an A100 GPU (batch size 128). Other values are taken from their papers.

Compressor	#Params↓	MACs↓	Speed (KB/s)↑	Multi Modal	bits/Byte↓							
					enwik9	Gutenberg	Spider	WikiSQL	GenoSeq	DNACorpus	LibriSpeech	
Classical	gzip† [52]	-	-	14500′	✓	2.590(0%)	3.819(0%)	2.289(0%)	1.672(0%)	2.390(0%)	2.318(0%)	6.511(0%)
	bzip2† [59]	-	-	3300′	✓	2.082	3.607	2.326	1.403	2.202	2.148	5.647
	zstd† [48]	-	-	11000′	✓	2.364	3.703	2.258	1.520	2.404	2.324	6.467
	FLAC† [18]	-	-	2000′	✗	-	-	-	-	-	-	4.961
Learning-based	Llama3*† [22]	8B	7.80G	20‡	✓	0.722	1.030	0.770	0.645	1.889	1.808	3.616
	RWKV*† [22]	7B	7.19G	86‡	✓	0.774	1.036	0.723	0.669	1.900	1.890	3.589
	tszip† [9]	169M	131M	180	✗	1.083	1.169	0.768	0.967	1.969	1.965	-
	NNCP† [8]	-	187M	1.6	✗	0.853	1.320	1.033	0.700	1.732	1.748	-
	CMIX† [38]	-	-	4	✗	0.879	1.363	1.056	0.629	1.656	1.667	-
	L3TC† [71]	12M	13.0M	580	✗	1.281	2.237	2.270	1.712	2.368	2.346	-
Ours	OmniZip-S	4.8M	3.88M	1223‡	✓	1.370(-47%)	1.552(-60%)	1.320(-42%)	1.170(-30%)	1.868(-24%)	2.015(-22%)	4.155(-36%)
	OmniZip-M	38M	18.2M	1015‡	✓	1.009(-61%)	1.278(-67%)	1.298(-43%)	0.842(-50%)	1.777(-26%)	1.810(-22%)	3.852(-41%)
	OmniZip-L	152M	56.0M	420‡	✓	0.980(-62%)	1.175(-69%)	1.243(-46%)	0.787(-53%)	1.740(-27%)	1.782(-23%)	3.810(-42%)

L further improve compression performance close to state-of-the-art levels, reaching 2.925, 0.987, and 3.937 bits/Byte on Kodak, TouchandGo, and Coronal datasets, respectively.

Compression Results on Text-like Data. Tab. 4 presents the lossless compression results on natural language, gene sequence, and database. Classical compressors like gzip, bzip2, and zstd achieve moderate performance (about 2.3 bits/Byte on enwik9, Spider, and GenoSeq). Learning-based text compressors perform strongly on natural language data, with NNCP and CMIX reaching 0.85 and 0.88 bits/Byte on enwik9. Pretrained LLMs compress natural language more effectively, but are computationally heavy and yield only modest gains on gene sequences.

OmniZip achieves competitive compression performance on these text-like datasets with much fewer parameters. OmniZip-S achieves about 24% to 47% performance gains compared to gzip across all text-like datasets. OmniZip-M and OmniZip-L, further enhance compression performance by another 10%~20%. The performance gains

on database and gene data are more pronounced, with OmniZip-L achieving near SOTA compression (1.740 and 1.782 bits/Byte) on GenoSeq and DNACorpus datasets.

Compression Results on Speech Data. As shown in Tab. 4, classical compressors such as gzip, bzip2, and zstd achieve 5.6~6.5 bits/Byte on LibriSpeech, while the specialized speech compressor FLAC performs better at 4.96 bits/Byte. Currently, there is no dedicated learning-based lossless speech compressor. The multi-modal method [22] provides promising compression (about 3.6 bits/Byte on LibriSpeech) but suffers from heavy complexity.

In contrast, OmniZip offers a superior balance between compression and efficiency, achieving 36%~42% improvements over gzip and 15~23% over FLAC on LibriSpeech.

4.3. Parameter and Complexity Analysis

We evaluate OmniZip’s inference speed across different hardware platforms and batch sizes, as shown in Fig. 5. The inference speed improves as the batch size increases

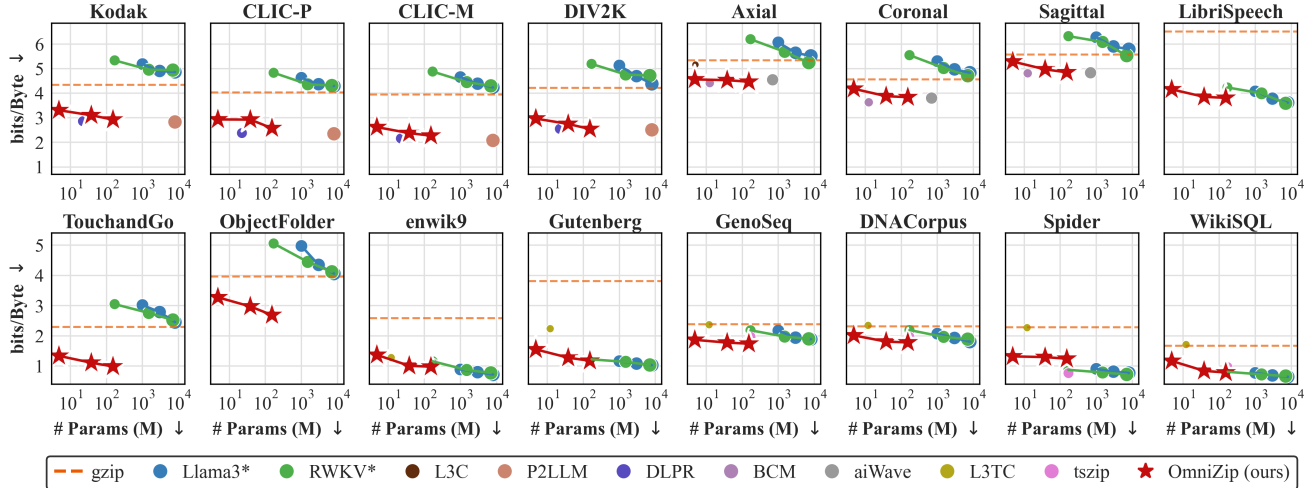


Figure 4. Comparison of learning-based lossless compressors across multi-modal datasets. The x-axis shows the model size (in millions of parameters), and the y-axis indicates compression efficiency (bits/Byte, lower is better). Models closer to the lower-left corner achieve better compression with fewer parameters. The dashed orange line represents the performance baseline of gzip.

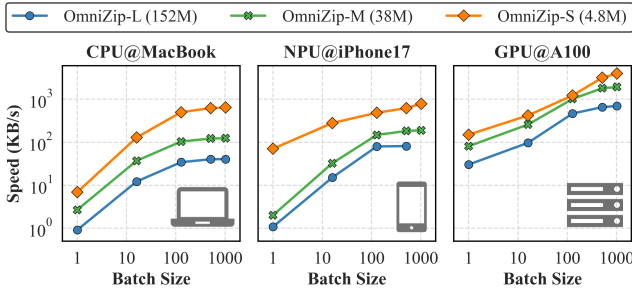


Figure 5. OmniZip’s inference speed across various platforms (CPU of MacBook Pro, NPU of iPhone17 Pro, and GPU of NVIDIA A100) and batch sizes (1, 16, 128, 512, 1024).

and saturates around a batch size of 512. Leveraging the modality-routing sparse design, OmniZip activates only a subset of parameters per token and achieves high computational efficiency. Specifically, on an NVIDIA A100 GPU, all three models achieve MB/s-level inference speeds, with OmniZip-S peaking at approximately 4MB/s. On resource-constrained devices like MacBook CPU and iPhone NPU, OmniComp-S achieves a near real-time speed of ~ 1 MB/s, and the larger variants reach up to ~ 200 KB/s.

Besides, we take OmniZip-S as an example to illustrate the routing patterns across modalities and modules, as shown in Fig. 6. Each bar represents the percent of expert activations for a given modality within a routing module (context learning or feedforward). We observe that context-learning routing exhibits more uneven expert utilization, where some experts may dominate specific modalities. In contrast, feedforward routing shows a more balanced expert usage, suggesting that contextual routing may capture more modality-specific dynamics, whereas feedforward routing tends to promote more generalized representation learning.

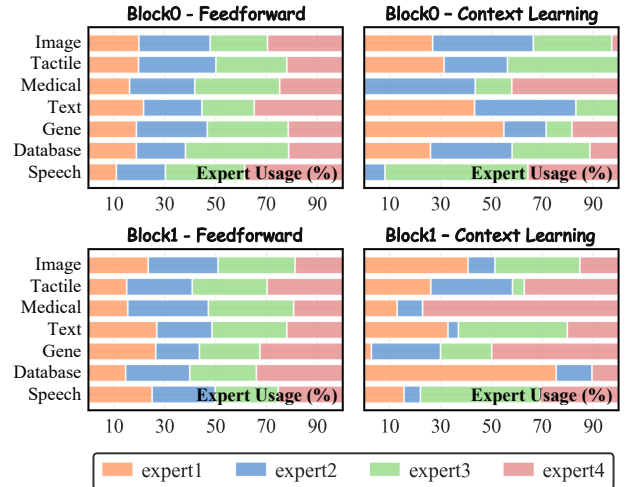


Figure 6. Expert usage of OmniZip-S across blocks and routing modules. Each bar shows the expert usage percent (%) for a modality in a routing module (context learning or feedforward).

4.4. Ablation Studies

Discussion on Multi-Modal Proposals. Tab. 5 reports ablations of our multi-modal components: the unified tokenizer enables multi-modality, while contextual and feed-forward routing provide modality adaptivity in context modeling and nonlinear transformation. We run all ablations on OmniZip-S with the same hyperparameters as the main experiments. It can be seen that removing either the routing mechanism leads to a clear drop in multi-modal compression performance, confirming their effectiveness in enhancing multi-modal compression.

Discussion on Modality-Routing Configurations. We analyze the configurations of the two modality-routing modules in contextual learning and feedforward stages.

Table 5. Ablations on all our proposals: modality-unified tokenization, modality-routing contextual learning, modality-routing feedforward, and reparameterization training. Compression performance (bits/Byte) is evaluated on representative dataset from each modality, and the inference speed is measured on a MacBook CPU with a batch size of 128. The chosen configuration is colored in orange.

Unified Tokenizer	Contextual Routing	Feedforward Routing	Reparam	Multi Modal	#Params↓	MACs↓	Speed _↓ (KB/s)↑	bits/Byte↓						
								Kodak	TouchandGo	Coronal	enwik9	Spider	GenoSeq	LibriSpeech
✗	✗	✗	✗	✗	3.2M	3.68M	856	-	-	-	1.658	-	-	-
✗	✗	✗	✓	✗	3.2M	3.68M	856	-	-	-	1.590	-	-	-
✓	✗	✗	✓	✓	3.2M	3.68M	856	3.383	1.453	4.545	1.660	1.662	1.984	4.365
✓	✗	✓	✓	✓	4.0M	3.73M	633	3.352	1.431	4.314	1.424	1.448	1.915	4.295
✓	✓	✗	✓	✓	3.0M	3.82M	780	3.339	1.419	4.188	1.410	1.482	1.889	4.302
✓	✓	✓	✗	✓	4.8M	3.88M	500	3.414	1.360	4.260	1.390	1.356	1.895	4.183
✓	✓	✓	✓	✓	4.8M	3.88M	500	3.307	1.338	4.179	1.370	1.320	1.868	4.155

Table 6. Ablations on modality-routing contextual learning. Routing is applied to all blocks with 4 experts and top- $k=2$. We report the total parameters and parameters activated per token. Compression performance (bits/Byte) is evaluated on representative dataset from each modality, and the inference speed is measured on a MacBook CPU with a batch size of 128. The chosen configuration is colored in orange.

Contextual Routing			#Params↓		MACs↓	Speed (KB/s)↑	bits/Byte↓						
Receptance	Key	Value	Total	Activated			Kodak	TouchandGo	Coronal	enwik9	Spider	GenoSeq	LibriSpeech
✓	✗	✗	4.8M	2.7M	3.88M	500	3.315	1.372	4.224	1.311	1.324	1.795	4.281
✗	✓	✗	4.8M	2.7M	3.88M	500	3.614	1.533	4.398	1.388	1.470	1.862	4.391
✗	✗	✓	4.8M	2.7M	3.88M	500	3.307	1.338	4.179	1.370	1.320	1.868	4.155
✓	✓	✗	5.4M	3.0M	4.02M	436	3.317	1.352	4.080	1.292	1.361	1.860	4.280
✓	✗	✓	5.4M	3.0M	4.02M	436	3.313	1.360	4.140	1.297	1.309	1.813	4.178
✗	✓	✓	5.4M	3.0M	4.02M	436	3.302	1.361	4.188	1.290	1.467	1.835	4.218
✓	✓	✓	6.0M	3.3M	4.17M	382	3.358	1.408	4.122	1.265	1.481	1.830	4.291

Table 7. Ablations on the configurations of the two modality-routing modules (e.g., routed blocks, expert count, top- k). We report the total parameters and parameters activated per token. Compression performance (bits/Byte) is evaluated on representative dataset from each modality, and the inference speed is measured on a MacBook CPU with a batch size of 128. The chosen configuration is colored in orange.

Blocks	top- k	Experts	Hidden Factor	#Params↓		MACs↓	Speed (KB/s)↑	bits/Byte↓						
				Total	Activated			Kodak	TouchandGo	Coronal	enwik9	Spider	GenoSeq	LibriSpeech
1	1	4	2×	3.6M	2.2M	3.65M	594	3.436	1.150	4.267	1.391	1.511	1.878	4.336
1	2	4	2×	3.6M	2.5M	3.85M	570	3.358	1.420	4.230	1.380	1.344	1.896	4.307
2	2	4	2×	4.8M	2.7M	3.88M	500	3.307	1.338	4.179	1.370	1.320	1.868	4.155
2	2	3	2×	4.0M	2.7M	3.88M	500	3.355	1.424	4.154	1.369	1.410	1.882	4.300
2	2	5	2×	5.2M	2.7M	3.88M	500	3.232	1.416	4.190	1.358	1.352	1.855	4.206
2	2	4	1×	3.2M	2.0M	3.48M	533	3.502	1.560	4.216	1.392	1.590	1.875	4.380
2	2	4	2×	4.8M	2.7M	3.88M	500	3.307	1.338	4.179	1.370	1.320	1.868	4.155
2	2	4	4×	8.0M	4.4M	4.65M	325	3.316	1.354	4.110	1.331	1.315	1.850	4.157

For contextual learning, we apply routing to different projection layers with 4 experts and top- k of 2. As shown in Tab. 6, applying routing to the V projection yields better compression performance than applying it to the K/R projections. Extending routing to more projections slightly increases model capacity but also leads to 10%~20% more parameters. Hence, we apply routing solely to the V projection in each contextual learning stage.

Then, we vary the number of routed blocks (from half to all), expert count (from 3 to 5), and top- k (from 1 to 2) for the contextual and feedforward routing modules, as shown in Tab. 7. It can be seen that using 4 experts and top- k of 2 yields the best trade-off between complexity and performance. We also vary the hidden factor of the feedforward routing module’s MLP experts. Moreover, setting the feedforward experts with a hidden factor of 2× strikes a good balance between compression performance and model compactness, hence it is adopted for OmniZip models.

5. Conclusion

We present OmniZip, a unified and lightweight lossless compressor designed for multi-modal data. It supports most

real-world data types suitable for lossless compression: image-like data (e.g., natural image, medical image, tactile signals), text-like data (e.g., natural language, gene sequence, database), and speech. Built on a lightweight backbone, OmniZip incorporates three components to enable efficient multi-modal compression: modality-unified tokenization, modality-routing context learning, and modality-routing feedforward. A reparameterization training strategy is also used to improve model capacity. OmniZip achieves compression performance on par with or better than existing state-of-the-art methods across multiple modalities, while using much fewer parameters. It also supports near real-time inference even on resource-constrained edge devices, like MacBook CPUs and iPhone NPUs.

6. Acknowledgments

This work was partly supported by the NSFC (62431015, 62571317, 62501387), the Fundamental Research Funds for the Central Universities, Shanghai Key Laboratory of Digital Media Processing and Transmission under Grant 22DZ2229005, 111 project BP0719010 and the Okawa Research Fund, the Ant Group Research Fund.

References

- [1] Hervé Abdi. Coefficient of variation. *Encyclopedia of research design*, 1(5), 2010. 5
- [2] Eirikur Agustsson and Radu Timofte. Ntire 2017 challenge on single image super-resolution: Dataset and study. In *Proceedings of the IEEE conference on computer vision and pattern recognition workshops*, pages 126–135, 2017. 5, 3
- [3] AI@Meta. Llama 3 model card. 2024. 1, 5
- [4] Ziya Arnavut. Move-to-front and inversion coding. In *Proceedings DCC 2000. Data Compression Conference*, pages 193–202. IEEE, 2000. 2
- [5] Yuanchao Bai, Xianming Liu, Kai Wang, Xiangyang Ji, Xiaolin Wu, and Wen Gao. Deep lossy plus residual coding for lossless and near-lossless image compression. *IEEE Transactions on Pattern Analysis and Machine Intelligence*, 46(5): 3577–3594, 2024. 1, 2, 5, 6, 4
- [6] Stefan Behnel, Robert Bradshaw, Craig Citro, Lisandro Dalcin, Dag Sverre Seljebotn, and Kurt Smith. Cython: The best of both worlds. *Computing in Science and Engineering*, 13(2):31–39, 2011. 3
- [7] Fabrice Bellard. Bpg image format. <https://bellard.org/bpg/>, 2014. Accessed: 2025-02-28. 2, 5, 6
- [8] Fabrice Bellard. NNCP v2: Lossless data compression with transformer. *Technical report, Amarisoft*, 2021. 1, 2, 5, 6
- [9] Fabrice Bellard. ts_zip: Text Compression using Large Language Models. https://bellard.org/ts_zip/, 2023. Accessed: 2024-08-10. 1, 2, 3, 5, 6, 4
- [10] Nicholas Bien, Pranav Rajpurkar, Robyn L Ball, Jeremy Irvin, Allison Park, Erik Jones, Michael Bereket, Bhavik N Patel, Kristen W Yeom, Katie Shpanskaya, et al. Deep-learning-assisted diagnosis for knee magnetic resonance imaging: development and retrospective validation of mrnet. *PLoS medicine*, 15(11):e1002699, 2018. 5, 3
- [11] Thomas Boutell. *PNG (Portable Network Graphics) Specification Version 1.0*. W3C, 1997. 2, 5, 6
- [12] Weilin Cai, Juyong Jiang, Fan Wang, Jing Tang, Sunghun Kim, and Jiayi Huang. A survey on mixture of experts. *arXiv preprint arXiv:2407.06204*, 2024. 4, 2
- [13] Kecheng Chen, Pingping Zhang, Hui Liu, Jie Liu, Yibing Liu, Jiaxin Huang, Shiqi Wang, Hong Yan, and Haoliang Li. Large language models for lossless image compression: Next-pixel prediction in language space is all you need. *arXiv preprint arXiv:2411.12448*, 2024. 1, 2, 3, 5, 6, 4
- [14] Zhengxue Cheng, Heming Sun, Masaru Takeuchi, and Jiro Katto. Learned image compression with discretized gaussian mixture likelihoods and attention modules. In *Proceedings of the IEEE/CVF conference on computer vision and pattern recognition*, pages 7939–7948, 2020. 2
- [15] Zhengxue Cheng, Yan Zhao, Keyu Wang, Li Song, and Hengdi ZHANG. Taco: A benchmark for lossless and lossy codecs of heterogeneous tactile data. In *The Fourteenth International Conference on Learning Representations*, 2026. 1
- [16] Clarivate Analytics. Geneseq™ database. <https://clarivate.com/intellectual-property/patent-intelligence/geneseq/>, 2024. Accessed: October 2025. 5, 3
- [17] CLIC. CLIC: Workshop and challenge on learned image compression. In *Proceedings of the IEEE/CVF Conference on Computer Vision and Pattern Recognition*, 2021. 5, 3
- [18] Josh Coalson. FLAC — free lossless audio codec. <https://xiph.org/flac/>, 2001. Version 1.0 released in 2001, maintained by Xiph.Org Foundation. 2, 5, 6
- [19] Wikipedia Community. enwik8: First 100m bytes of the english wikipedia dump. <https://cs.fit.edu/~mmahoney/compression/enwik8.zip>, 2006. Pre-processed version used for character-level language modeling benchmarks. 3, 5
- [20] Wikipedia Community. enwik9: Complete english wikipedia dump (xml). <https://cs.fit.edu/~mmahoney/compression/enwik9.zip>, 2007. Full Wikipedia XML dump preprocessed for large-scale language modeling. 3, 5
- [21] Eastman Kodak Company. Kodak lossless true color image suite. Internal Research Dataset, 1999. 24 uncompressed PNG images, 768x512 resolution. 5, 3
- [22] Gregoire Deletang, Anian Ruoss, Paul-Ambroise Duquenne, Elliot Catt, Tim Genewein, Christopher Mattern, Jordi Grau-Moya, Li Kevin Wenliang, Matthew Aitchison, Laurent Orseau, Marcus Hutter, and Joel Veness. Language modeling is compression. In *The Twelfth International Conference on Learning Representations*, 2024. 1, 2, 3, 5, 6, 4
- [23] Xiaohan Ding, Xiangyu Zhang, Ningning Ma, Jungong Han, Guiguang Ding, and Jian Sun. Repvgg: Making vgg-style convnets great again. In *Proceedings of the IEEE/CVF conference on computer vision and pattern recognition*, pages 13733–13742, 2021. 3, 2
- [24] Junhao Du, Chuqin Zhou, Ning Cao, Gang Chen, Yunuo Chen, Zhengxue Cheng, Li Song, Guo Lu, and Wenjun Zhang. Large language model for lossless image compression with visual prompts. *arXiv preprint arXiv:2502.16163*, 2025. 1, 2, 3
- [25] Zhihao Du, Shiliang Zhang, Kai Hu, and Siqi Zheng. Fun-codec: A fundamental, reproducible and integrable open-source toolkit for neural speech codec. In *ICASSP 2024-2024 IEEE International Conference on Acoustics, Speech and Signal Processing (ICASSP)*, pages 591–595. IEEE, 2024. 2
- [26] Jarek Duda. Asymmetric numeral systems: entropy coding combining speed of Huffman coding with compression rate of arithmetic coding. *arXiv:1311.2540*, 2013. 1
- [27] Donghui Feng, Zhengxue Cheng, Shen Wang, Ronghua Wu, Hongwei Hu, Guo Lu, and Li Song. Linear attention modeling for learned image compression. In *Proceedings of the Computer Vision and Pattern Recognition Conference*, pages 7623–7632, 2025. 2
- [28] Ruohan Gao, Yen-Yu Chang, Shivani Mall, Li Fei-Fei, and Jiajun Wu. Objectfolder: A dataset of objects with implicit visual, auditory, and tactile representations. *arXiv preprint arXiv:2109.07991*, 2021. 5, 3

- [29] Google. Webp image format. <https://developers.google.com/speed/webp>, 2010. Accessed: 2025-02-28. 2, 5, 6
- [30] Michael J Gormish and J Allen. Finite state machine binary entropy coding. In *Proc. Data Compression Conference*, page 449. Citeseer, 1993. 2
- [31] Albert Gu and Tri Dao. Mamba: Linear-time sequence modeling with selective state spaces. *arXiv preprint arXiv:2312.00752*, 2023. 3, 1
- [32] David Heurtel-Depeiges, Anian Ruoss, Joel Veness, and Tim Genewein. Compression via pre-trained transformers: A study on byte-level multimodal data. *arXiv preprint arXiv:2410.05078*, 2024. 1, 2
- [33] Paul G. Howard and Jeffrey Scott Vitter. Analysis of arithmetic coding for data compression. In *Proceedings of Data Compression Conference (DCC)*, 1991. 1, 3
- [34] David A. Huffman. A method for the construction of minimum-redundancy codes. In *Proceedings of the IRE*, 1952. 1, 2
- [35] Wonseok Hwang, Jinyeong Yim, Seunghyun Park, and Minjoon Seo. A comprehensive exploration on wikisql with table-aware word contextualization. *arXiv preprint arXiv:1902.01069*, 2019. 5, 3
- [36] Apple Inc. Core ml, 2023. Apple’s framework for integrating machine learning models into apps. 3
- [37] ISO/IEC. Jpeg 2000 image coding system. <https://www.jpeg.org/jpeg2000/>, 2000. Accessed: 2025-02-28. 2, 5, 6
- [38] Byron Knoll. Cmix version 20, a lossless data compression program. <http://www.byronknoll.com/cmixon.html>, 2023. Accessed: 2024-08-10. 1, 2, 5, 6
- [39] Siu Kwan Lam, Antoine Pitrou, and Stanley Seibert. Numba: A llvm-based python jit compiler. In *Proceedings of the Second Workshop on the LLVM Compiler Infrastructure in HPC*, pages 1–6, 2015. 3
- [40] Yang Li, Yan Zhao, Zhengxue Cheng, and Hengdi Zhang. Taccompress: A benchmark for multi-point tactile data compression in dexterous manipulation. *arXiv preprint arXiv:2505.16289*, 2025. 2
- [41] Jinming Liu, Heming Sun, and Jiro Katto. Learned image compression with mixed transformer-cnn architectures. In *Proceedings of the IEEE/CVF conference on computer vision and pattern recognition*, pages 14388–14397, 2023. 2
- [42] Xiangrui Liu, Meng Wang, Shiqi Wang, and Sam Kwong. Bilateral context modeling for residual coding in lossless 3d medical image compression. *IEEE Transactions on Image Processing*, 33:2502–2513, 2024. 1, 2, 5, 6, 4
- [43] Ilya Loshchilov and Frank Hutter. Sgdr: Stochastic gradient descent with warm restarts. *arXiv preprint arXiv:1608.03983*, 2016. 5
- [44] Huidong Ma, Sun Hui, Liping Yi, Ding Yanfeng, Gang Wang, et al. Msdzip: Universal lossless compression for multi-source data via stepwise-parallel and learning-based prediction. In *THE WEB CONFERENCE 2025*. 1
- [45] Giovanni Manzini. An analysis of the burrows—wheeler transform. *Journal of the ACM (JACM)*, 48(3):407–430, 2001. 2
- [46] Fabian Mentzer, Eirikur Agustsson, Michael Tschannen, Radu Timofte, and Luc Van Gool. Practical full resolution learned lossless image compression. In *Proceedings of the IEEE/CVF Conference on Computer Vision and Pattern Recognition (CVPR)*, pages 10629–10638, 2019. 1, 2, 5, 6, 4
- [47] Fabian Mentzer, Luc Van Gool, and Michael Tschannen. Learning better lossless compression using lossy compression. In *Proceedings of the IEEE/CVF conference on computer vision and pattern recognition*, pages 6638–6647, 2020. 2, 5, 6
- [48] Meta. ZSTD, Zstandard - Fast real-time compression algorithm. <https://github.com/facebook/zstd>, 2015. Accessed: 2024-08-10. 2, 5, 6
- [49] Fazal Mittu, Yihuan Bu, Akshat Gupta, Ashok Devireddy, Alp Eren Ozdarendeli, Anant Singh, and Gopala Anumanchipalli. Finezip: Pushing the limits of large language models for practical lossless text compression. *arXiv preprint arXiv:2409.17141*, 2024. 2, 3
- [50] NVIDIA. Apex (a pytorch extension). <https://nvidia.github.io/apex/optimizers.html>, 2018. API Documentation for NVidia’s Apex optimizers. 5
- [51] Vassil Panayotov, Guoguo Chen, Daniel Povey, and Sanjeev Khudanpur. Librispeech: an asr corpus based on public domain audio books. In *2015 IEEE international conference on acoustics, speech and signal processing (ICASSP)*, pages 5206–5210. IEEE, 2015. 5, 3
- [52] Richard C. Pasco. GZIP file format specification version 4.3. *RFC 1952*, 1996. 2, 5, 6
- [53] Bo Peng, Eric Alcaide, Quentin Anthony, et al. Rvk: Re-inventing rnn for the transformer era, 2023. Accessed: 2024-08-10. 5
- [54] Bo Peng, Ruichong Zhang, Daniel Goldstein, Eric Alcaide, Haowen Hou, Janna Lu, William Merrill, Guangyu Song, Kaifeng Tan, Saiteja Utpala, et al. Rvk-7” goose” with expressive dynamic state evolution. *arXiv preprint arXiv:2503.14456*, 2025. 3, 4, 1, 2
- [55] Diogo Pratas and Armando J Pinho. A dna sequence corpus for compression benchmark. In *International Conference on Practical Applications of Computational Biology & Bioinformatics*, pages 208–215. Springer, 2018. 5, 3
- [56] Project Gutenberg. Project gutenber corpus. 2013. Available at: <https://www.gutenberg.org/>. 5, 3
- [57] Hassan Ramchoun, Youssef Ghanou, Mohamed Ettaouil, and Mohammed Amine Janati Idrissi. Multilayer perceptron: Architecture optimization and training. 2016. 4, 1
- [58] Rico Sennrich, Barry Haddow, and Alexandra Birch. Neural machine translation of rare words with subword units, 2016. Accessed: 2024-08-10. 3, 1
- [59] Julian Seward. On the Performance of BWT Sorting Algorithms. *Proceedings of the IEEE Data Compression Conference 2000*, 2000. 2, 5, 6
- [60] C. E. Shannon. A mathematical theory of communication. *The Bell System Technical Journal*, 27(3):379–423, 1948. 1
- [61] N Shazeer, A Mirhoseini, K Maziarz, A Davis, Q Le, G Hinton, and J Dean. The sparsely-gated mixture-of-experts layer. *Outrageously large neural networks*, 2, 2017. 4

- [62] Jon Sneyers. Flif - free lossless image format. <https://flif.info/>, 2015. Accessed: 2023-10-01. 2, 5, 6
- [63] JPEG XL Team. Jpeg xl image coding system. <https://jpeg.org/jpegxl/>, 2021. Accessed: 2025-02-28. 2, 5, 6
- [64] Chandra Shekhara Kaushik Valmeekam, Krishna Narayanan, Dileep Kalathil, Jean-Francois Chamberland, and Srinivas Shakkottai. Llmzip: Lossless text compression using large language models. *arXiv preprint arXiv:2306.04050*, 2023. 1, 2, 3
- [65] Ashish Vaswani, Noam Shazeer, Niki Parmar, Jakob Uszkoreit, Llion Jones, Aidan N. Gomez, Lukasz Kaiser, and Illia Polosukhin. Attention is all you need, 2017. Accessed: 2024-08-10. 3, 1
- [66] Jun Xu, Zhengxue Cheng, Guangchuan Chi, Yuhan Liu, Yuelin Hu, and Li Song. Rate-aware learned speech compression. In *2025 IEEE International Symposium on Circuits and Systems (ISCAS)*, pages 1–5. IEEE, 2025. 2
- [67] Dongmei Xue, Haichuan Ma, Li Li, Dong Liu, and Zhiwei Xiong. Aiwave: Volumetric image compression with 3-d trained affine wavelet-like transform. *IEEE Transactions on Medical Imaging*, 42(3):606–618, 2022. 1, 2, 5, 6, 4
- [68] Fengyu Yang, Chenyang Ma, Jiacheng Zhang, Jing Zhu, Wenzhen Yuan, and Andrew Owens. Touch and go: Learning from human-collected vision and touch. *arXiv preprint arXiv:2211.12498*, 2022. 5, 3
- [69] Xiaoxuan Yang, Guo Lu, Donghui Feng, Zhengxue Cheng, Guosheng Yu, and Li Song. Coarse-to-fine transformer for lossless 3d medical image compression. In *2024 IEEE International Conference on Visual Communications and Image Processing (VCIP)*, pages 1–5. IEEE, 2024. 2
- [70] Tao Yu, Rui Zhang, Kai Yang, Michihiro Yasunaga, Dongxu Wang, Zifan Li, James Ma, Irene Li, Qingning Yao, Shanella Roman, et al. Spider: A large-scale human-labeled dataset for complex and cross-domain semantic parsing and text-to-sql task. *arXiv preprint arXiv:1809.08887*, 2018. 5, 3
- [71] Junxuan Zhang, Zhengxue Cheng, Yan Zhao, Shihao Wang, Dajiang Zhou, Guo Lu, and Li Song. L3tc: Leveraging rkv for learned lossless low-complexity text compression. In *Proceedings of the AAAI Conference on Artificial Intelligence*, pages 13251–13259, 2025. 1, 2, 3, 5, 6, 4
- [72] Shifeng Zhang, Ning Kang, Tom Ryder, and Zhenguo Li. iflow: Numerically invertible flows for efficient lossless compression via a uniform coder. *Advances in Neural Information Processing Systems*, 34:5822–5833, 2021. 2
- [73] Shifeng Zhang, Chen Zhang, Ning Kang, and Zhenguo Li. ivpf: Numerical invertible volume preserving flow for efficient lossless compression. In *Proceedings of the IEEE/CVF Conference on Computer Vision and Pattern Recognition*, pages 620–629, 2021. 2
- [74] Yan Zhao, Zhengxue Cheng, Junxuan Zhang, Qunshan Gu, Qi Wang, and Li Song. Dualcomp: End-to-end learning of a unified dual-modality lossless compressor. *arXiv preprint arXiv:2505.16256*, 2025. 1
- [75] Yan Zhao, Yang Li, Zhengxue Cheng, Hengdi Zhang, and Li Song. Taccompress: A benchmark for multi-point tactile data compression in dexterous hand. In *Proceedings of the 1st International Workshop on Multi-Sensorial Media and Applications*, pages 54–62, 2025. 1
- [76] Abraham Ziv, Jacob; Lempel. A Universal Algorithm for Sequential Data Compression. *IEEE Transactions on Information Theory*, 1977. 2
- [77] Barret Zoph. Designing effective sparse expert models. In *2022 IEEE International Parallel and Distributed Processing Symposium Workshops (IPDPSW)*, pages 1044–1044. IEEE, 2022. 4

OmniZip: Learning a Unified and Lightweight Lossless Compressor for Multi-Modal Data

Supplementary Material

The supplementary material includes deeper explanations of the proposed method and extended experiments, covering: (1) detailed descriptions of the modality-unified tokenization, modality-routing context learning, modality-routing feedforward design, and reparameterization training strategy; (2) implementation details of multi-modal datasets and training/testing process; (3) extended lossless compression performance using adjusted bits/Byte as the metric.

7. Backbone Selection

We compare three common backbone architectures for the probability prediction model: Transformer [65], Mamba [31], and RWKV [54]. These models are evaluated in terms of compression efficiency (bits/Byte), computational cost (MACs), and inference speed (KB/s).

As for Transformer, We use a causal, decoder-only Transformer implemented in JAX/Haiku. Input tokens are embedded, scaled, and summed with sinusoidal positional encodings, then processed through a stack of eight multi-head self-attention (8 heads) and feed-forward layers, each followed by residual connections and LayerNorm. For Mamba and RWKV, we adopt their official implementations¹². The trained models are converted into CoreML packages and benchmarked on a MacBook Pro 2024 with an Apple M4 chip using CPU inference.

8. Modality-Unified Tokenization

To enable multi-modal lossless compression, we design a reversible modality-unified tokenization strategy that maps heterogeneous data into a shared token space. The main challenge arises from the fundamentally distinct structures of different modalities. Moreover, to ensure lossless reconstruction, the tokenization process must be fully invertible.

For text-like data, including natural language, gene sequences, and databases, we follow [71] and adopt a SentencePiece BPE tokenizer [58] with a vocabulary size of 16K. To better adapt to domain-specific characteristics, we extend the vocabulary with symbolic tokens: like nucleotide bases (A, T, G, C) for gene sequences, and common SQL keywords (e.g., SELECT, FROM, WHERE) for databases. Formally, given a text string S , the tokenizer performs:

$$S_{\text{text}} \xrightarrow{\text{SPM BPE}} [x_1, x_2, \dots, x_n], \quad x_i \in \mathcal{V}_{\text{text}}, |\mathcal{V}_{\text{text}}| = 16\text{K}. \quad (4)$$

¹Mamba: <https://github.com/state-spaces/mamba>.

²RWKV: <https://github.com/BlinkDL/RWKV-LM>.

For image-like data, including natural, medical, and tactile images, we partition each image into $16 \times 16 \times 3$ patches to preserve local spatial correlations. Pixels within each patch are flattened in raster-scan order, and each RGB channel is expanded sequentially: $[R_1, G_1, B_1, R_2, G_2, B_2, \dots]$. We treat each 8-bit sub-pixel as an independent token (i.e., $|\mathcal{V}_{\text{image}}| = 256$), thereby maintaining inter-pixel and inter-channel correlations. For grayscale medical images, each 8-bit intensity value is directly mapped to a single token. Tactile data are handled in two ways: visual tactile maps are processed as regular RGB images, while 3D tactile force vectors (x, y, z) are linearly mapped into pseudo-RGB triplets for tokenization.

Speech is continuous and hard to discretize without loss. Hence, we adopt a next-byte prediction scheme, reading the raw byte stream and treating each byte as a token:

$$S_{\text{speech}}(t) \xrightarrow{\text{each byte}} [x_1, x_2, \dots, x_n], \quad x_i \in [0, 255], \quad (5)$$

yielding a 256-size vocabulary shared with image-like modalities (i.e., $|\mathcal{V}_{\text{speech}}| = 256$).

After tokenization, we merge all modality vocabularies into a single unified token space:

$$\mathcal{V}_{\text{uni}} = \mathcal{V}_{\text{text}} \cup \mathcal{V}_{\text{image}} \cup \mathcal{V}_{\text{speech}}. \quad (6)$$

Each sequence is prefixed with a modality identifier token, i.e., <image>, <medical>, <tactile>, <text>, <gene>, <database>, or <speech>, allowing the model to learn modality-aware priors during probability estimation.

Before softmax and arithmetic coding, we apply modality-specific masking to restrict the active token probabilities and improve the compression efficiency. For example, during image compression, only tokens in $\mathcal{V}_{\text{image}}$ are retained, and all others are zeroed out:

$$p_{\text{image}}(x_i | x_{<i}) = \text{softmax}(o(x_i | x_{<i}) \odot M_{\text{image}}), \quad (7)$$

where M_{image} is a binary mask selecting image tokens, $o(x_i | x_{<i})$ is the output logit before softmax.

9. Modality-Routing Context Learning

As shown in Fig. 7, each RWKV block [54] consists of two components: a Time Mixing module and a multilayer perceptron (MLP) [57]. The Time Mixing module serves as a lightweight alternative to attention, modeling contextual dependencies through a recurrent formulation. Instead of computing pairwise attention, it maintains a running state that summarizes past tokens, allowing linear-time inference.

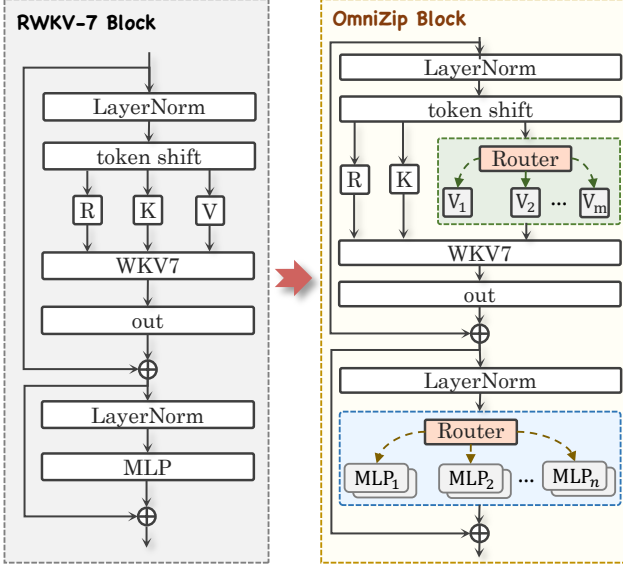


Figure 7. Key structural differences between RWKV-7 and OmniZip model. Left: an RWKV-7 block. Right: an OmniZip block.

As stated, different modalities exhibit distinct contextual dependencies. For instance, text are one-dimensional sequential and have mostly short-range semantic dependencies. Images are two-dimensional and flattened into sequences, with inter-pixel and inter-channel correlations. Speech is continuous and temporally structured.

To enhance multi-modal adaptability, we integrate a mixture-of-experts (MoE) mechanism [12] into the Time Mixing module. MoE dynamically selects specialized experts based on input tokens, enabling conditional computation and reducing unnecessary activation. Specifically, given an input token x_i , a router network predicts a score:

$$g_{i,e} = \text{softmax}(x_i \cdot W_g)_e = \frac{\exp(x_i \cdot W_{g,e})}{\sum_{e'=1}^E \exp(x_i \cdot W_{g,e'})}, \quad (8)$$

where E is the expert count, W_g is the routing projection. $g_{i,e}$ means the likelihood that expert e should process x_i .

To keep efficiency, we adopt top- k sparse routing, where only the experts with top- k highest scores are activated, and their outputs are aggregated as a weighted sum. We experiment with applying MoE to different components and find that the V layer benefits most from such adaptive routing. Conceptually, the K layer serves as a semantic index, and the R layer acts as a temporal gate, while the V layer encodes concrete contextual content. Allowing diversity in V layer enables the model to adapt more flexibly to modality-specific information. Hence, we apply MoE only to the V layer, sharing K and R layers across all V experts. Formally,

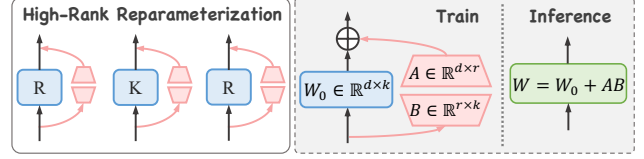


Figure 8. Illustration of the reparameterization training strategy.

the V-projection output in our MoE design is computed as:

$$V(x_i) = \sum_{e \in \text{top-}k} \hat{g}_{i,e} e(x_i), \quad (9)$$

where each expert e is a distinct V projection layer, and $\hat{g}_{i,e}$ denotes the re-normalized routing score.

To ensure model compactness, we use $E = 4$ experts and $k = 2$. This setup increases the number of parameters by only three additional V layers per Time Mixing module, yet notably improves the multi-modal adaptability.

10. Modality-Routing Feedforward

In the RWKV backbone [54], each block integrates a feed-forward MLP that projects intermediate representations into a higher-dimensional space, applies nonlinear transformations, and fuses contextual information from the Time Mixing module. This structure enhances model expressiveness but treats all tokens uniformly, regardless of their modality. In fact, a single shared MLP is insufficient to capture the distinct properties of heterogeneous modalities.

To better support multi-modal compression, we replace this MLP with a modality-routing feedforward module based on MoE. The routing mechanism follows the design in Sec. 9, while the experts here are small MLPs instead of V layers. Each MLP expert adopts a hidden factor of $2\times$, half that of the original large MLP. With four experts and top- $k = 2$, the number of activated parameters per token remains nearly identical to the original design.

11. Reparameterization Training Strategy

Following [71], we adopt a high-rank reparameterization training strategy to enhance OmniZip’s compression capacity without increasing inference complexity. During training, each R, K, and V projection layer in the Time Mixing module is augmented with an auxiliary high-rank branch to improve representational power. At inference, these auxiliary branches are merged back into the main path through structural reparameterization, maintaining a compact single-path design, as illustrated in Fig. 8.

Specifically, instead of using parallel branches like 1×1 convolutions or shortcuts as in [23], we follow the strategy in [71] and reparameterize each branch as a product of two high-rank matrices: $A \in \mathbb{R}^{d \times r}$ and $B \in \mathbb{R}^{r \times k}$, where the

Table 8. Details of the utilized multi-modal datasets (16 datasets from 7 modalities).

Dataset	Type	Train	Test	Description
Kodak [21]	image	✗	✓	24 film-scanned photos (768 × 512) with balanced natural and synthetic scenes. We use it for testing.
CLIC-P [17]	image	✗	✓	41 high-resolution DSLR images (mostly 2K) with rich color and texture diversity. We use it for testing.
CLIC-M [17]	image	✗	✓	61 smartphone photos (mostly 2K) containing real-world noise and artifacts. We use it for testing.
DIV2K [2]	image	✓	✓	900 2K-resolution images with a large diversity of contents. We follow the official split (800 train, 100 test).
Axial [10]	medical	✓	✓	2D knee MRI slices (256 × 256) in the axial plane. We follow the official split (~38K train, ~4.1K test).
Coronal [10]	medical	✓	✓	2D knee MRI slices (256 × 256) in the coronal plane. We follow the official split (~33K train, ~3.5K test).
Sagittal [10]	medical	✓	✓	2D knee MRI slices (256 × 256) in the sagittal plane. We follow the official split (~34K train, ~3.6K test).
TouchandGo [68]	tactile	✓	✓	A tactile dataset of 140 trajectories (640 × 480), with 60% for training and the rest for testing.
ObjectFolder [28]	tactile	✓	✓	A tactile dataset of 1000 trajectories (120 × 160), with 60% for training and the rest for testing.
enwik8 [19]	text	✓	✗	The first 100MB of the English Wikipedia dump. We use it for testing.
enwik9 [20]	text	✗	✓	The first 1GB of the English Wikipedia dump. We use it for testing.
Gutenberg [56]	text	✓	✓	A library containing 75K eBooks. We randomly select 2K and 1K books for training and testing, respectively.
GenoSeq [16]	gene	✓	✓	17 genomics sequencing dataset with FastQ format. We use 10 for training and 7 for testing.
DNACorpus [55]	gene	✓	✓	DNA sequences of 15 species, we follow the official split (370MB for training and 246MB for testing).
Spider [70]	database	✓	✓	5693 SQL queries on 200 databases. We follow the official split (314MB for training and 60MB for testing).
WikiSQL [35]	database	✓	✓	24241 SQL queries from Wikipedia. We follow the official split (38MB for training and 12MB for testing).
LibriSpeech [51]	speech	✓	✓	A 1000-hour English speech dataset. We follow the official split (1GB for training and 600MB for testing).

main-path’s weight is $W_0 \in \mathbb{R}^{d \times k}$ and $r \gg d, k$. During training, the layer’s output is the sum of the main branch and the bypass branch. These branches are merged at inference via structural reparameterization: $W = W_0 + A \times B$, resulting in a single-path structure that reduces both runtime and memory usage. Importantly, although the branches are merged during inference, the learned multi-branch parameters are preserved, maintaining high capability.

In OmniZip, this strategy is applied to all the R/K/V layers in the Time Mixing module. Following [71], we set the decomposition rank r to $4 \times$ the embedding dimension.

12. Multi-Modal Datasets

We conduct experiments across seven data types, including natural images, medical images, tactile signals, text, gene sequences, databases, and speech, covering a total of 16 datasets for training and evaluation, as shown in Tab. 8.

To ensure balanced and stable multi-modal training, we normalize the data scale across modalities by restricting each modality’s training set to approximately 1 GB. For large datasets, samples are randomly drawn to maintain representative coverage of content diversity, while smaller datasets are augmented through simple transformations such as random cropping/flipping, token shuffling, or noise perturbation (depending on the modality type).

During training, we also adopt a balanced batch sampling strategy to prevent overfitting toward some modalities. Specifically, the dataloader cycles through all modalities in a round-robin manner, dynamically constructing each batch by uniformly sampling from the shuffled indices of every modality. This ensures that each batch contributes an equal number of samples per modality, allowing the model

to learn modality-invariant patterns.

Regarding the model input format, as stated in Sec. 8, for image-like data, each input corresponds to a flattened $16 \times 16 \times 3$ patch, resulting in a sequence length of 768 tokens. Text-like and speech data are processed as sequential streams, with each input sequence containing 1024 tokens.

13. Training and Testing Process

To accelerate the overall pipeline, we incorporate optimizations like Cython [6], Numba [39], and distributed parallelization. For model evaluation and deployment, we test OmniZip across three hardware platforms: (1) NVIDIA A100 GPU (for training and high-throughput testing), (2) MacBook Pro 2024 (Apple M4 CPU), and (3) iPhone 17 Pro (A19 NPU). For CPU and NPU evaluation, we convert the trained PyTorch models into CoreML packages [36] and conduct profiling via Xcode Instruments. For GPU evaluation, we switch the GPU to performance mode and ensure no other processes are running on the device. We then measure inference latency by executing the model 1000 times consecutively and report the average runtime.

14. Adjusted Compression Results

To provide a more realistic evaluation of deployment efficiency, we adopt the adjusted bits-per-Byte metric, which incorporates model size into the compressed data size. It penalizes large models and reflects the trade-off between compression performance and model storage overhead.

As shown in Tab. 9 and Tab. 10, OmniZip-S achieves superior adjusted compression efficiency across all seven modalities, including image-like, text-like, and speech

Table 9. Adjusted compression performance (bits/Byte) on image-like (natural image, medical image, and tactile) datasets. * denotes pretrained LLMs, † indicates that some results are reproduced by us. Other values are taken from their papers.

Compressor	#Params↓	Multi Modal	Adjusted bits/Byte↓								
			Kodak	CLIC-P	CLIC-M	DIV2K	TouchandGo	ObjectFolder	Axial	Coronal	Sagittal
Llama3*† [22]	8B	✓	8490321	971320	553618	291465	322642	214197	693352	750368	970961
RWKV*† [22]	7B	✓	7429031	849906	484417	255032	282312	187423	606683	656573	823341
DLPR*† [5]	22.3M	✗	23670	2710	1545	815	900	601	-	-	-
L3C*† [46]	5M	✗	5310	610	349	185	203	138	439	473	594
P2LLM [13]	8B	✗	8490319	971318	553616	291463	-	-	-	-	-
aiWave [67]	695M	✗	-	-	-	-	-	-	59372	64254	80574
BCM [42]	12.5M	✗	-	-	-	-	-	-	1088	1176	1475
OmniZip-S	4.8M	✓	5097	586	335	178	195	132	421	454	570
OmniZip-M	38M	✓	40332	4618	2632	1387	1534	1020	3298	3568	4475
OmniZip-L	152M	✓	161319	18458	10521	5540	6131	4072	13178	14261	17883

Table 10. Adjusted compression performance (bits/Byte) on text-like (natural language, gene sequence, database) and speech datasets. * denotes pretrained LLMs, † indicates that some results are reproduced by us. Other values are taken from their papers.

Compressor	#Params↓	Multi Modal	Adjusted bits/Byte↓						
			enwik9	Gutenberg	Spider	WikiSQL	GenoSeq	DNACorpus	LibriSpeech
Llama3*† [22]	8B	✓	129	362459	2125	10835	500	1138	212
RWKV*† [22]	7B	✓	113	317152	1859	9480	437	996	186
tszip [9]	169	✗	4	7658	46	230	13	26	-
L3TC [71]	12	✗	2	546	6	18	3	4	-
OmniZip-S	4.8M	✓	1	219	3	8	2	3	4
OmniZip-M	38M	✓	2	1723	11	52	4	7	5
OmniZip-L	152M	✓	3	6888	42	207	11	23	8

datasets. OmniZip-M and OmniZip-L also exhibit satisfactory balance between compression efficiency and deployability. Among modality-specific compressors, Mentzer et al. [46] and Zhang et al. [71] achieve competitive adjusted compression efficiency on image-like and text-like datasets, respectively. Though [22] demonstrate strong compression efficiency on text-like and speech datasets, their massive parameter sizes dominate the total compression cost, resulting in significantly higher adjusted bits-per-Byte values.